Coastal morphological monitoring using an automated video system at Praia de Faro (South Portugal)

Vousdoukas, M.V. (1), Almeida, L.P(1)., Ferreira, Ó. (1), Taborda, R. (2), Silva, A.N.(2).

(1) University of Algarve, CIMA – Centre of Marine and Environmental Research
(2) University of Lisbon – Faculty of Sciences

ABSTRACT:
An automated video system is presented for coastal morphological monitoring consisting of 2 IP cameras and a PC, acquiring imagery from the coastal zone during 10 min every hour during daylight, with an acquisition frequency of 1 Hz. The system is used to monitor a coastal section 500 m alongshore Praia de Faro with resolution varying from 0.2 m to 3 m and is programmed to generate snapshot, time averaged (timex), variance and timestack images on an hourly basis. Automatic shoreline extraction algorithms were developed and combined with real time wave and tidal measurements produce intertidal topographic impressions for each tidal cycle. Comparison with RTK-GPS topographic surveys showed RMS errors ranging from 10 to 20 cm and the information is used to update a DTM, which along with wave run up measurements are the major direct system products.

KEYWORDS: beach erosion, video monitoring, coastal morphodynamics, sediment transport, wave run up

1. INTRODUCTION

The EU project Morphological Impacts and Coastal Risks by Extreme storm events (MICORE) aims to develop and demonstrate on-line tools for reliable predictions of the morphological impact of marine storm events in support of civil protection mitigation strategies. The project is specifically targeted to contribute to the development of a probabilistic mapping of the morphological impact of marine storms and to the production of early warning and information systems to support long-term disaster reduction.

Monitoring of nine selected case-study sites at equal European countries is taking place to assess the impact of the storms on living and non-living resources will be assessed and real-time warning systems will be designed and proposed for implementation to National Civil Protection agencies. The most important end product is the production of risk indicators with defined threshold for the identification of major morphological changes and flooding associated vulnerability.

Praia de Faro, Algarve is the Portuguese study site for the project, located in the Southern Portuguese coast. The study site is a mesotidal (tidal range ~3 m) reflective beach with very dynamic morphodynamic behavior. Significant wave heights up to 5 m during storm events are being recorded on an annual basis and the erosion are recovery rates have been shown to be very fast.

Against this background, an Automated video system was developed and installed at the beach, aiming to follow the rapid morphodynamic changes taking place at the study site.

2. THE VIDEO SYSTEM

2.1 General description

2 IP cameras were installed on a 4 m tall metallic structure, placed on the top of Paquete restaurant and the total elevation of the center of view (COV) is ~20 above sea level. Both cameras are connected to a PC and are acquiring imagery from the coastal zone during 10 min every hour during daylight, with an acquisition frequency of 1 Hz.

Figure 1. The cameras at Praia de Faro

The system is used to monitor a coastal section 500 m alongshore with resolution varying from 0.2 m to 3 m and is programmed to execute scheduled image processing operations, so as to generate snapshot, time averaged (timex), variance and timestack images on an hourly basis. Timex images are 10 min averaged images where the white patterns can be used as proxies for wave breaking and shoreline locations. The above features are often more clearly displayed on the timex images which show the 10 variance of the pixel intensities along the image. Finally, timestack images show the swash shoreward limit position along a cross-shore transect, during

the 10 mins period and along with topographic data, can provide wave run up heights.

2.2 Image geo-rectification

The key processing required for this application is the accurate rectification of the obtained imagery, projecting the scenes and objects with image coordinates (U, V) to a horizontal plane in real world, metric system coordinates (X, Y, Z). This procedure is called geo-rectification and is here performed utilizing homogenous coordinates using the 3x4 perspective transformation matrix *P* (Hartley and Zisserman, 2006):

$$P\begin{bmatrix} X \\ Y \\ Z \\ 1 \end{bmatrix} = \begin{bmatrix} U \\ V \\ 1 \end{bmatrix} \qquad 1$$

The *P* matrix can be decomposed as:

$$P = K\,R\,[I\,|{-C}] \qquad 2$$

where *K* is an upper triangular matrix, known as the camera calibration matrix (e.g. see Bouguet, 2007), *I* is the identity matrix, and *C* and *R* are the translation and rotation matrices of the camera's center of view respectively (Hartley and Zisserman, 2006).

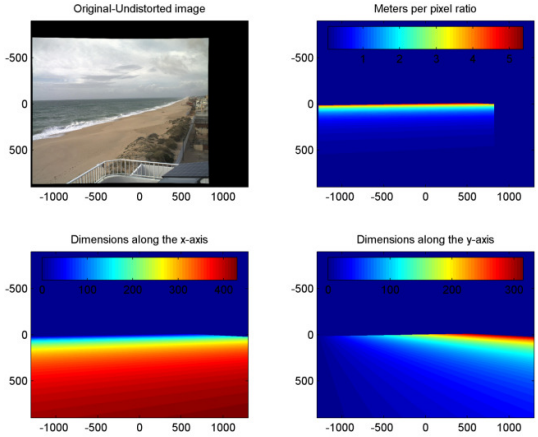

Figure 2. From upper left to lower right: Example of an undistorted snaphot image; geospatial transformations of pixel dimension: meters per pixel ratio, x and y real world dimensions (m), displayed in the image space.

K matrix determination takes place using standard procedures well explained in the literature (e.g. see Bouguet, 2007), while the *C* translation matrix accounts for the location of the camera center of view (COV) in the world coordinate reference system:

$$C = \begin{bmatrix} X_{cam} \\ Y_{cam} \\ Z_{cam} \end{bmatrix} \qquad 3$$

R matrix expresses the effective orientation of the camera imaging plane and is defined by three angles, the COV-pan, COV-tilt and COV-roll, relative to the Cartesian system of coordinates (e.g. Hartley and Zisserman, 2006; Holland and Holman, 1997; Vousdoukas et al., 2009a).

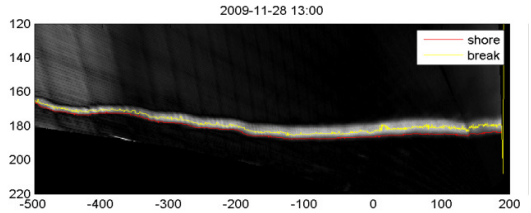

Figure 3. Georectified SIGMA image (the system is rotated by ~37 degress). Red and yellow lines correspond to the automatically extracted shoreline and break line position

A set of points with known image and world coordinates was considered (Ground Control Points, from now on called GCPs) to be introduced in an iterative solver to estimate P, from Equations 1, 2 and 3 (e.g. Lippmann and Holman, 1989). According to all the above, 3 GCPs are sufficient to define the camera geometry and position, while additional ones result in an over-specified system permitting the selection of an optimal solution, estimated through an iterative solver (Nelder-Mead Simplex Method, see Lagarias et al., 1998).

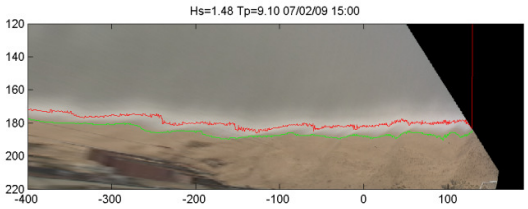

Figure 4. Georectified TIMEX image (the system is rotated by ~37 degress). Green and red lines correspond to the automatically extracted shoreline and break line position

2.3 Image processing

Automatic shoreline extraction algorithms were developed combining colour segmentation, on the timex images, and pixel intensities criteria, on the variance images. The elevation of the extracted shorelines is obtained from wave run up height formulations, using as input off-shore wave and tidal measurements, as well as the beach face slope, updated daily from the system. The level of breaking positions is provided by a wave propagation model

(Vousdoukas et al., 2009b) run on the latest available topo-bathymetric profile from the area.
Since both features are being extracted every hour, several contours can be accumulated on a daily basis. Those data after post-processing are used to extract the current intertidal topography and update a Digital Terrain Model of Praia de Faro.

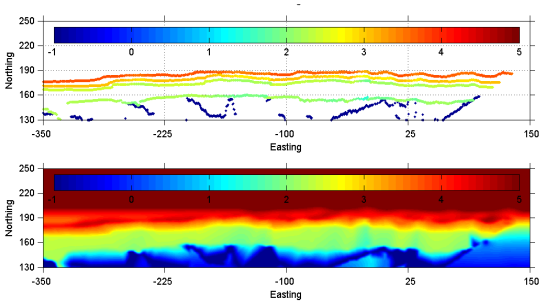

Figure 5. Example of the Digital Terrain Model update operations. Upper panel: the resulting contour from image acquisition/processing during a tidal cycle. Lower panel: The updated DTM

3. RESULTS-DISCUSSION

The system is designed to run real time, with image geo-referencing based on a DTM in an effort to reduce geo-location errors from object shadowing. The latter is constantly updated from the remote sensed topography, as well as from regular field surveys which also serve for validation and updating of other-than-intertidal sections. Comparison of the remotely sensed topography with RTK-GPS topographic surveys showed RMS errors ranging from 10 to 20 cm.

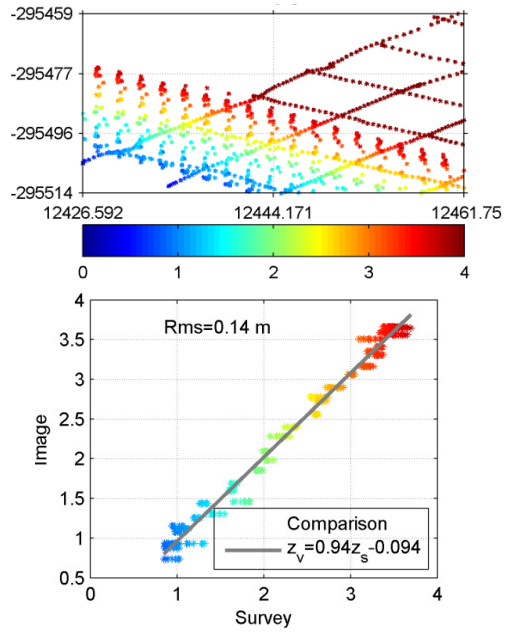

Figure 6. Example of remotely sensed intertidal topography validation. Upper panel: video sensed points superimposed to the RTK DGPS grid obtained the same day (bigger grid); colormap expresses elevation. Lower panel: Scatter comparison plot

Intense effort has been devoted to test and optimize different system set-ups, in order to make it self-sustained. The computer is constantly connected on the internet and is using a two repositories of software and additional data (camera calibration and geo-rectification parameters, products, etc), with two other computers on the university campus.

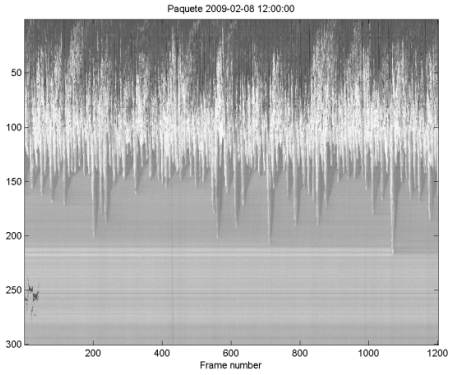

Figure 7. Timestack image. x-axis corresponds to acquired frames (time) and y to cross-shore distance

The system is programmed to take into consideration lack-of, or rogue data, as well as bad quality imagery, using input quality and other operational criteria. It has been also optimized for the specific site conditions and to produce wave and topographic information, after conducting automatic output quality control and uploads information on an FTP part of which can be accessed at http://w3.ualg.pt/~mvousdoukas/video_system.html. Moreover, the amount of data produced are invaluable for process interpretation and are being used to obtain new, more accurate parameterizations of wave characteristics (e.g. more accurate site specific wave run up formulations). The above are then incorporated in the system, and the interactions above, coupled with the whole architecture constitute a highly complex and non-linear set of operations. Given the above, the automatic video system is an ideal platform for artificial intelligence and machine learning techniques, which are currently tested.

4. REFERENCES

Bouguet, J.-Y., 2007. Camera Calibration Toolbox for Matlab, pp. http://www.vision.caltech.edu/bouguetj/calib_doc/.

Hartley, R. and Zisserman, A., 2006. Multiple View Geometry in Computer Vision. Cambridge University Press.

Holland, K.T. and Holman, R.A., 1997. Video estimation of foreshore topography using

trinocular stereo. Journal of Coastal Research SI, 13: 81-87.

Lagarias, J.C., Reeds, J.A., Wright, M.H. and Wright, P.E., 1998. Convergence Properties of the Nelder-Mead Simplex Method in Low Dimensions. SIAM Journal of Optimization, 9(1): 112-147.

Lippmann, T.C. and Holman, R.A., 1989. Quantification of sand bar morphology: A video technique based on wave dissipation. Journal of Geophysical Research, 94(C1): 995-1011.

Vousdoukas, M.I., Velegrakis, A.F., Dimou, K., Zervakis, V. and Conley, D.C., 2009a. Wave run-up observations in microtidal, sediment-starved pocket beaches of the Eastern Mediterranean. Journal of Marine Systems, 78: 37-47.

Vousdoukas, M.I., Velegrakis, A.F. and Karambas, T.V., 2009b. Morphology and sedimentology of a microtidal, beachrock-infected beach: Vatera Beach, Lesvos, NE Mediterranean. Continental Shelf Research, 29: 1937-1947.